JACS
JOURNAL OF THE AMERICAN CHEMICAL SOCIETY

COMMUNICATION

pubs.acs.org/JACS

A Bottom-Up Approach To Fabricate Patterned Surfaces with Asymmetrical TiO_2 Microparticles Trapped in the Holes of Honeycomblike Polymer Film

Xiaofeng Li,[†,‡] Liang Zhang,[†,‡] Yongxin Wang,[†,‡] Xiaoli Yang,[†,‡] Ning Zhao,[*,†] Xiaoli Zhang,[†] and Jian Xu[*,†]

[†]Beijing National Laboratory for Molecular Sciences, State Key Laboratory of Polymer Physics and Chemistry, Institute of Chemistry, Chinese Academy of Sciences, Beijing 100190, P.R. China

[‡]Graduate University of Chinese Academy of Sciences, Beijing 100049, P.R. China

Supporting Information

ABSTRACT: Patterned "bead in pore" composite film with hemispherical or mushroomlike TiO_2 microparticles lying in the holes of a honeycomblike polystyrene matrix has been fabricated by a template-free bottom-up approach from a homogeneous solution of $TiCl_4$/polystyrene/$CHCl_3$ using the breath figures method. It is a very simple way to prepare hemispherical or mushroomlike TiO_2 microparticles and to get the hexagonally nonclose-packed arrays of asymmetrical particles with or without polymer matrix, which have potential applications in photonics.

Microparticles are of considerable interest because of their extensive applications in optics,[1] controlled release,[2] biomedical fields,[3] and so on. These applications depend on the chemical and physical properties of the particles, such as wettability, size, and shape, which are also important for their self-assembly.[4] Recently, there has been great interest in the synthesis of colloidal particles with specific asymmetric structures and their assembly, since such systems are valuable in the creation of complex structures through anisotropic interactions,[5] which have unique photonic properties.[6] Hemispherical and mushroomlike microparticles are typical asymmetrical particles that have promising applications in photonics[7] and other fields.[8] Because of the minimization of interfacial tension energy, microparticles tend to adopt the spherical shape via a nucleation growth manner.[9] Asymmetrical structures are rarely prepared by a self-growth process, especially hemispherical and mushroomlike structures. Complicated methods such as seeding polymerization[10] and microfluidics[11] are commonly used to prepare polymeric particles with hemispherical or mushroomlike shapes. These methods, however, are not applicable for the inorganic particles, which need more complicated procedures and rigorous conditions.[12] Compared to the more easily obtained asymmetrical polymeric particles, inorganic particles with high refractive index have more outstanding properties for application in a special area.[13] Therefore, it is important to find an easy and versatile method to prepare asymmetrical inorganic particles.

Patterning of microparticles is another important issue for their applications.[5c] Template-assisted self-assembly[9] was an effective way to construct colloid aggregates with complex and controllable architectures in the holes of the template.[14] However, formation of this "bead-in-pore" morphology needs at least two steps: fabrication of the template and assembly of the colloids. In addition, most colloids used in self-assembly are spherical particles. It is difficult for asymmetrical particles to assemble into well-defined, complex supra-particular structures, because the "hard" asymmetrical particles are unstable in water due to the lack of electrostatic or steric stabilization effects.[15] Computational studies demonstrate that ordered morphologies should be experimentally accessible for asymmetrical structures.[16] However, to achieve these goals remains challenging.

Herein we report a very simple and template-free bottom-up approach to fabricate a patterned "bead-in-pore" composite film with hemispherical or mushroomlike TiO_2 filling in the holes of honeycomblike polystyrene (PS) matrix from a homogeneous solution of $TiCl_4$/PS/$CHCl_3$ by the breath figures (BFs) method.[17] Water droplet arrays condensed on the solution surface acted as the "microreactors" for the hydrolysis of $TiCl_4$, and at the same time PS self-organized around the arrays of "microreactors" to form an ordered porous matrix. The in situ formed hydrolyzing product took a hemispherical or mushroomlike shape after solidification, depending on the concentration of the precursor in the solution; thus, inorganic/polymer composite patterned film with one particle in one hole was obtained. The asymmetrically shaped TiO_2 particles and the porous polymer film can be obtained by selectively removing the counterpart from the composite film. More interestingly, hexagonally nonclose-packed arrays analogous to that of the insect compound eyes can be formed by peeling the hemispherical particles off the composite film with an adhesive tape.

Figure 1a shows a typical morphology of the resultant film from evaporation of $TiCl_4$/PS/$CHCl_3$ solution (PS, 1 wt %, $TiCl_4$, 0.2% v/v) cast on glass. A highly ordered topology with particles trapped in the holes of the porous film can be observed. The holes and particles are arranged hexagonally with few defects. The average diameter of the pores is about 1.9 μm, while the size of the particles inside is a little smaller. Gaps between particles and holes can be observed. This ordered film is strongly iridescent. Perception of the color shifts from green through purple to yellow by varying the angle of observation of the obtained surface. When a laser with a beam diameter of 1 mm was irradiated on the film, the diffraction image projected on a screen showed a hexagonal diffraction pattern (inset of Figure 1a), demonstrating a long range of ordered structure on the film. SEM image of the cross section (Figure 1b) shows that the film has a single-layer porous structure

Received: November 28, 2010

dx.doi.org/10.1021/ja1106767 | J. Am. Chem. Soc. XXXX, XXX, 000–000

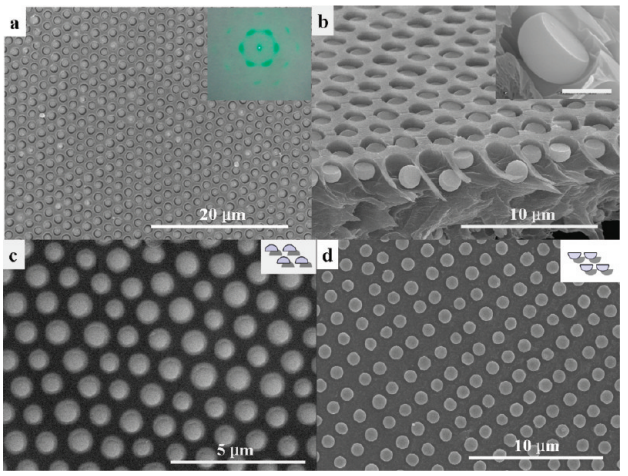

Figure 1. SEM images of (a) top and (b) cross section of the ordered composite film, (c) the hexagonally nonclose-packed hemispherical particles array adhered to the adhesive tape, (d) the hemispherical particles array on glass after removal of PS by calcination. Inset in (a) is the diffraction pattern of the film irradiated by a laser pointer. Inset in (b) is the magnified hemispherical particle with a scale bar of 1 μm. Insets in (c) and (d) are the schemes of the particle arrays.

on the surface, and more interestingly, the particle in the hole is hemispheric. Peeling the hemispherical particles off the composite film with an adhesive tape, we can get hexagonally nonclose-packed arrays of the hemispherical particles (Figure 1c). Because the particles adhere to the adhesive layer with different depth, depending on the force employed on each of the particles during peeling, the perimeters of the particles exhibited are not uniform. This morphology is analogous to the compound eyes of insects, which has aroused great research interest in photonics.[8a]

On the other hand, after calcining the composite film on glass at 450 °C, an ordered array of hemispherical particles with flat faces exposed can be obtained on glass, with a little change of the arrangement in the porous polymer matrix (Figure 1d). It has been demonstrated that, compared to the spherical colloids consisting of photonic crystals, the asymmetrical building blocks can lift the symmetry-induced degeneracy of photonic bands, leading to complete photonic band gaps in face-centered cubic and other simple lattices,[18] which would provide enhanced light control.[19]

More interestingly, the shape of the particles can be easily tuned by adjusting the concentration of $TiCl_4$ and PS. When the concentration of PS was fixed at 1 wt %, large-scale ordered structures could be obtained with the $TiCl_4$ concentration in the range 0.2−0.4% (v/v). When the $TiCl_4$ concentration was < 0.3% (v/v), hemispherical particles were obtained (Figure 1), whereas in the range 0.3−0.4% (v/v), the resultant particles were mushroomlike (Figure 2). In addition, the size of the mushroomlike particles decreased with increasing $TiCl_4$ concentration. It was difficult to get an ordered structure when the concentration of $TiCl_4$ was > 0.4% (v/v). On the other hand, when PS concentration was 0.7 wt % and $TiCl_4$ concentration was 0.2% (v/v), we could get particles with concave surfaces, the dimple particles (Figure S1, Supporting Information (SI)).

The hexagonal pattern is typical of BFs phenomena.[20] However, different from traditional BFs methods in which high relative humidity (RH) or the moist flow is necessary for the formation of ordered structure, the regular pattern in our system was obtained at a RH of 20−50%. The low RH preparation and the novel "particle in hole" pattern can be ascribed to the composition of the beginning

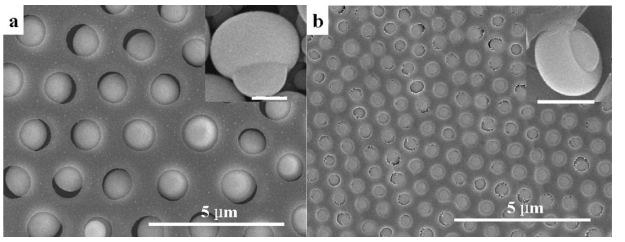

Figure 2. SEM images of the obtained composite film from the $TiCl_4$/PS/$CHCl_3$ solution with different concentrations of $TiCl_4$: (a) 0.3% v/v and (b) 0.4% v/v. (PS, 1 wt %, RH, 30%) Insets in (a) and (b) are the magnified mushroomlike particles, respectively. Scale bar = 0.5 μm.

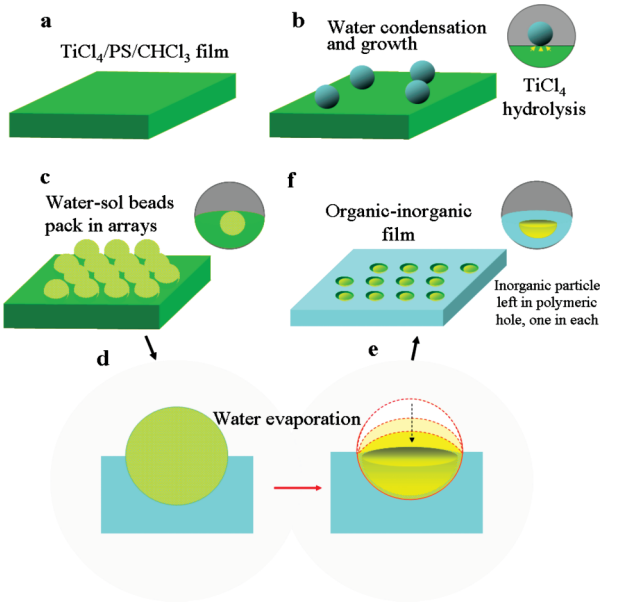

Figure 3. Scheme of formation of the highly ordered asymmetrical inorganic particle/polymer composite films by BFs method.

solution, which contains polymer and strong hydrolyzable precursor as well. Several phenomena take place simultaneously during solvent evaporation of the precursor/polymer solution, including condensation and arrangement of water droplets, hydrolysis of $TiCl_4$ when coming into contact with water, and self-assembly of polymer around the liquid arrays,[20] as schematically shown in Figure 3.

When the $TiCl_4$/PS/$CHCl_3$ solution is cast on glass slide, the volatile $CHCl_3$ evaporates quickly (Figure 3a). Because of the evaporative cooling effect, water droplets are condensed on the cold solution surface (Figure 3b).[20] Meanwhile $TiCl_4$ begins to hydrolyze in the presence of water. The hydrolysis product is more likely the intermediate salt of $Ti(OH)_nCl_{4-n}$ due to the limited amount of water and reaction time (discussed in detail later).[21] The intermediate product will diffuse in the water droplets because of its higher affinity with water. As a result, inorganic sol droplets are formed instead of the pure water droplets in traditional BFs methods. The sol droplets float on the solution and arrange hexagonally to obtain the lowest free energy. Meanwhile, the polymer chains assemble around the droplets (Figure 3c). After complete evaporation of $CHCl_3$, sol-droplet arrays are immobilized in polymer matrix (Figure 3d). In traditional BFs process, the later evaporation of water droplets left behind empty holes in the film, whereas in our case, the droplets are "reservoirs" of the hydrolysis product of $TiCl_4$.

dx.doi.org/10.1021/ja1106767 |J. Am. Chem. Soc. XXXX, XXX, 000–000

Further evaporation of water in the sol droplets will result in condensation of the sol, leading to formation of inorganic particles in the hole. Because the sol-droplet arrays float on the surface of the polymer matrix (see SEM images in Figure 1b), it is more likely that the projecting part of the droplet in the air shrinks gradually with the three-phase contact line fixed at the air−sol−polymer matrix (Figure 3e), similar to sessile water drop evaporation on solid surface.[22] Further loss of water will lead the condensed sol droplets to become gel-like and finally to form the solid particles (Figure 3f). The final shape of the particle depends on the concentration of hydrolysis product in the sol droplet. For medium concentration, the solidified product takes the shape of the cavity of the matrix. However, if more or less $TiCl_4$ is involved, the resultant particle will have a papilla or concave shape compared with the hemisphere, and thus, mushroomlike or dimple particles are formed. For the mushroomlike particles, we find that the size of the pore is nearly the same as the diameter of the papilla. During the evaporation process, more than half of the sol droplet sinks in the polymer solution and is surrounded by the aggregated polymer. It is commonly regarded that evaporation of the water happens after evaporation of the solvent. While the polymer may not be totally solidified during water evaporation, the size of the three-phase contact line can change. If there is a convex above the three-phase contact line when the sol changes to gel-like, the two sides of the sol droplet that lie above and below the three-phase contact line can contract, respectively, accompanied with a little shrinking of the three-phase contact line, forming the mushroomlike particles. We prepare the dimple particles from the solution with 0.7 wt % PS, 0.2% $TiCl_4$ (v/v). Compared with the solution for the hemispherical particles that has 1 wt % PS, 0.2% $TiCl_4$ (v/v), lower polymer concentration in the BFs method would induce larger water droplets.[23] The concentration of hydrolysis product in the sol droplets from 0.7 wt % PS solution would be smaller than that from 1 wt % PS solution when other conditions are identical, and the obtained particles would have a concave surface. Therefore, ordered arrays of different asymmetrical microparticles can be produced from a very simple evaporation process.

The composition of particles in the composite film is complicated, since hydrolysis of $TiCl_4$ is a step-by-step process.[24] Hydrolyzation will give rise to substitution of Cl^- by OH^- and formation of HCl and $Ti(OH)_nCl_{4-n}$ (n = 1,2,3,4, SI). This hydrolysis can be completed rapidly when enough water is involved at high temperature, otherwise intermediate product is formed.[21] During the evaporation process, the condensed water was scanty and the temperature was relatively low, as a result, the hydrolysis did not proceed completely. XPS investigation demonstrated that the Cl/Ti molar ratio of the freshly prepared composite film (Figure 1a) was about 1.3, indicating the hydrolysis yield was the mixture of $Ti(OH)_2Cl_2$ and $Ti(OH)_3Cl$. When the freshly prepared composite film was subjected to water, the particles could be washed away, leaving behind the highly ordered porous PS films (Figure S2, SI). The aqueous suspension with dispersed particles had a strong UV absorbance starting at 350 nm (Figure S3, SI). Drying the aqueous suspension left a bulk aggregate instead of hemispherical particles, indicating again that the freshly prepared hemisphere in the composite film was intermediate salts which could continue hydrolysis in water. This continual hydrolysis also could be completed slowly when the composite film was kept in ambient conditions. The intermediate product combined with vapor phase H_2O, and hydrolysis was continued; finally the intermediate product converted to TiO_2, and the steady, ordered TiO_2/PS composite film was achieved (Table S1, SI). The intermediate product can be transformed to anatase TiO_2 by calcining the composite film at

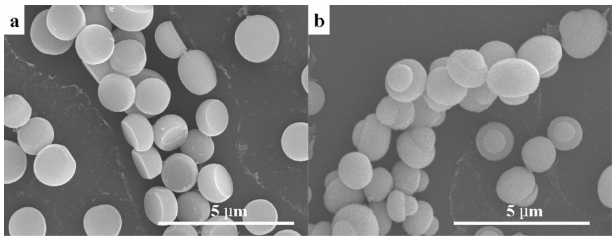

Figure 4. SEM images of (a) hemispherical and (b) mushroomlike TiO_2 microparticles after calcination of the composite film at 450 °C for 3 h.

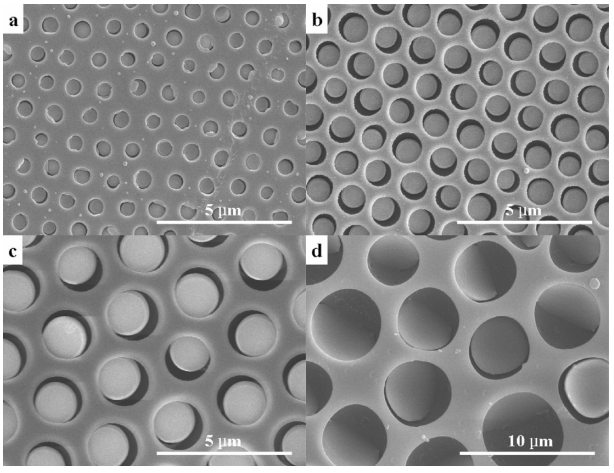

Figure 5. SEM images of the as-formed composite films obtained at RH of (a) 20%, (b) 30%, (c) 50%, and (d) 70%.

450 °C for 3 h (Figure 4). XRD investigation proves the particles are amorphous before calcination but anatase after (Figure S4a, SI). XPS spectra show the calcined sample has a peak at 458.7 eV, which corresponds to $2p_{3/2}$ of Ti in TiO_2 (Figure S4b, SI), while the freshly prepared hemispherical particles in the composite film have a peak at 460.1 eV, characteristic of the hydroxyl chloride intermediates.[25] The Ti $2p_{3/2}$ peak had little change when the composite films were obtained from the $TiCl_4$/PS/$CHCl_3$ solution with different $TiCl_4$ concentrations. When other conditions were identical, the Ti $2p_{3/2}$ binding energy increased with increasing $TiCl_4$ concentration, because more Cl^- was left in the particles. So the mushroomlike particles have a higher Ti $2p_{3/2}$ binding energy than hemispherical particles before calcination, but after calcination, the particles are anatase TiO_2 without any chloride, and Ti in both kinds of particles has the same binding energy (Figure S4c, SI).

The size of the particles can be easily tuned by changing the evaporation conditions. Figure 5 shows the dependence of the morphology on the RH. The SEM images show that the pore size of the film increases with RH. When the solution is 0.1 wt % PS, 0.2% $TiCl_4$ (v/v), the average diameters of the pores are about 0.6, 1.1, and 1.9 μm at RH of 20, 30, and 50%, respectively. The particle size also increases with increasing RH. The pores and particles are not monodisperse but have narrow polydispersity.[23] The size distribution of the calcined hemispherical particles in Figure 1d is shown in Figure S5 (SI). The pores are arranged less regularly at RH of 70% and are filled with tabletlike particles (Figure 5d and Figure S6a, (SI)). This irregular order at high RH is mainly due to coagulation of the rapidly condensing droplets, leading to a dramatic increase of the droplet size and size distribution.[26] The concentration of the

dx.doi.org/10.1021/ja1106767 |J. Am. Chem. Soc. XXXX, XXX, 000–000

hydrolysis product in the droplet is relatively low, leading to the formation of wafery tablets.

The facts that ordered BFs structure can be obtained at low RH and show a dependence on $TiCl_4$ concentration clearly demonstrate that adding $TiCl_4$ in the solution assists the formation of an ordered structure. The reason may be that hygroscopic $TiCl_4$ promotes the growth of the water droplets at low RH and the resultant sol droplets are large enough for ordered arrangement as the template.[27] When the $TiCl_4$ concentration is <0.2% (v/v), the promotion is not enough, and the ordered structure cannot be obtained. $TiCl_4$ concentration >0.3% (v/v) may induce more nucleation of the condensed water, and many more, but smaller, pores and particles are formed. When too much $TiCl_4$ (>0.4% (v/v)) is involved, the hydrolysis product coalesces together and prohibits formation of the ordered structure. Transference and hydrolysis of the precursor at the water/solution interface may also form a protective layer to stabilize the droplets from coalescence. In control experiments, flat PS film was obtained by casting the PS/$CHCl_3$ solution under the same condition (20−50% RH), while porous PS film with big and irregular holes was formed at higher RH (Figure S6b,c (SI)). Therefore, two benefits can be expected by adding the precursor in the solution: the strong water-absorbent property of $TiCl_4$ promotes formation of droplet arrays at low RH; the as-formed sol templates are easy to prevent from coagulating. Thus, polymers without special architecture or composition can be used. In our system, hydrolysis of $TiCl_4$ is confined in the droplet arrays, leaving the particles to take the shape of the cavity of the pore. Previously reported polymer/precursor system only had honeycomblike films with inorganic nanoparticles enriched on the wall of the pore by BFs method.[14b,28] Our result is also different from that reported by Jiang et al. where only spherical microspheres were obtained when the precursor was hydrolyzed in the spherical pores of polymer film.[29] Herein we show for the first time the fabrication of asymmetrical inorganic particles lying in the hole of honeycomblike polymer film by a bottom-up approach. It is a very simple way to prepare hemispherical and mushroomlike TiO_2 microparticles, and realize the patterned structure of nonspherical particles. It is versatile so asymmetrical particles also can be produced when PS is substituted by other polymers such as poly(ethyl α-cyanoacrylate) and polycarbonate (Figure S7, (SI)).

In conclusion, we have described a simple bottom-up approach to fabricate ordered composite film with hemispherical or mushroomlike TiO_2 particles lying in the holes of honeycomblike PS film from the $TiCl_4$/PS/$CHCl_3$ solution via BFs method. By separating the organic or inorganic components of the composite film, honeycomblike PS film and TiO_2 microparticles can be obtained, respectively, and hexagonal nonclose-packed TiO_2 hemisphere arrays will be formed by peeling the particles off the film with an adhesive trap. This method is versatile: other polymers also can be employed, and other hemispherical or mushroomlike particles may be obtained by using corresponding precursors. This method opens a new way to fabricate asymmetrical inorganic particles and their ordered arrays, which may find applications in photonic crystal, biomedicine, catalysis, and so on.

■ ASSOCIATED CONTENT

Supporting Information. Experimental procedures, XRD and XPS spectra, and SEM images. This material is available free of charge via the Internet at http://pubs.acs.org.

■ AUTHOR INFORMATION

Corresponding Author
zhaoning@iccas.ac.cn; jxu@iccas.ac.cn

■ ACKNOWLEDGMENT

This work was supported by the NSFC (Nos. 50803072, 50821062), 973 Project (2009AA033601) and CAS Innovation Project (No. 2007CB936400).

■ REFERENCES

(1) (a) Wong, S.; Kitaev, V.; Ozin, G. A. *J. Am. Chem. Soc.* **2003**, *125*, 15589–15598. (b) Redl, F. X.; Cho, K. S.; Murray, C. B.; O'Brien, S. *Nature* **2003**, *423*, 968–971.
(2) Petros, R. A.; Ropp, P. A.; DeSimone, J. M. *J. Am. Chem. Soc.* **2008**, *130*, 5008–5009.
(3) Caruso, F. *Colloids and Colloid Assemblies*; Wiley-VCH: Weinheim,Germany, 2004.
(4) (a) Dendukuri, D.; Doyle, P. S. *Adv. Mater.* **2009**, *21*, 4071–4086. (b) Choi, C.-H.; Lee, J.; Yoon, K.; Tripathi, A.; Stone, H. A.; Weitz, D. A.; Lee, C.-S. *Angew. Chem., Int. Ed.* **2010**, *49*, 7914–7918.
(5) (a) Feyen, M.; Weidenthaler, C.; Schuth, F.; Lu, A. H. *J. Am. Chem. Soc.* **2010**, *132*, 6791–6799. (b) Sun, Q.; Wang, Q.; Jena, P.; Kawazoe, Y. *ACS Nano* **2008**, *2*, 341–347. (c) Glotzer, S. C.; Solomon, M. J. *Nat. Mater.* **2007**, *6*, 557–562.
(6) (a) Kim, J. W.; Larsen, R. J.; Weitz, D. A. *J. Am. Chem. Soc.* **2006**, *128*, 14374–14377. (b) Roh, K. H.; Martin, D. C.; Lahann, J. *Nat. Mater.* **2005**, *4*, 759–763.
(7) (a) Jayabalan, J.; Singh, M. P.; Banerjee, A.; Rustagi, K. C. *Phys. Rev. B* **2008**, *77*, 045421. (b) Nam, H. J.; Jung, D. Y.; Yi, G. R.; Choi, H. *Langmuir* **2006**, *22*, 7358–7363. (c) Heremans, P.; Genoe, J.; Kuijk, M.; Vounckx, R.; Borghs, G. *IEEE Photonics Technol. Lett.* **1997**, *9*, 1367–1369.
(8) (a) Jeong, K. H.; Kim, J.; Lee, L. P. *Science* **2006**, *312*, 557–561. (b) del Campo, A.; Greiner, C.; Arzt, E. *Langmuir* **2007**, *23*, 10235–10243.
(9) Xia, Y. N.; Yin, Y. D.; Lu, Y.; McLellan, J. *Adv. Funct. Mater.* **2003**, *13*, 907–918.
(10) Tanaka, T.; Komatsu, Y.; Fujibayashi, T.; Minami, H.; Okubo, M. *Langmuir* **2010**, *26*, 3848–3853.
(11) (a) Nie, Z.; Xu, S.; Seo, M.; Lewis, P. C.; Kumacheva, E. *J. Am. Chem. Soc.* **2005**, *127*, 8058–8063. (b) Nisisako, T.; Torii, T. *Adv. Mater.* **2007**, *19*, 1489–1493.
(12) (a) Li, Y.; Sasaki, T.; Shimizu, Y.; Koshizaki, N. *Small* **2008**, *4*, 2286–2291. (b) Su, Y. W.; Wu, C. S.; Chen, C. C.; Chen, C. D. *Adv. Mater.* **2003**, *15*, 49–51.
(13) Joannopoulos, J. D.; Meade, R. D.; Winn, J. N. *Photonic Crystals*; Princeton University Press: Princeton, NJ, 1995.
(14) (a) Van Blaaderen, A.; Ruel, R.; Wiltzius, P. *Nature* **1997**, *385*, 321–324. (b) Lu, M. H.; Zhang, Y. *Adv. Mater.* **2006**, *18*, 3094–3098.
(15) Suzuki, D.; Tsuji, S.; Kawaguchi, H. *J. Am. Chem. Soc.* **2007**, *129*, 8088–8089.
(16) Hosein, I. D.; Liddell, C. M. *Langmuir* **2007**, *23*, 8810–8814.
(17) Widawski, G.; Rawiso, M.; Francois, B. *Nature* **1994**, *369*, 387–389.
(18) (a) Xia, Y. N.; Gates, B.; Li, Z. Y. *Adv. Mater.* **2001**, *13*, 409–413. (b) Leung, K. M.; Liu, Y. F. *Phys. Rev. Lett.* **1990**, *65*, 2646–2649.
(19) Noda, S.; Yokoyama, M.; Imada, M.; Chutinan, A.; Mochizuki, M. *Science* **2001**, *293*, 1123–1125.
(20) Srinivasarao, M.; Collings, D.; Philips, A.; Patel, S. *Science* **2001**, *292*, 79–83.
(21) Rigo, M.; Canu, P.; Angelin, L.; Della Valle, G. *Ind. Eng. Chem. Res.* **1998**, *37*, 1189–1195.
(22) Birdi, K. S.; Vu, D. T. *J. Adhes. Sci. Technol.* **1993**, *7*, 485–493.
(23) Bunz, U. H. F. *Adv. Mater.* **2006**, *18*, 973–989.
(24) (a) Shinkarev, A. N.; Shtrambrand, Y. M.; Shaulov, Y. K.; Andreeva, N. I.; Ryabenko, E. A. *Zh. Fiz. Khim.* **1973**, *47*, 2945. (b) Chen, R. C. *Hydrometall. China* **1999**, *3*, 1–6.
(25) Groenen, B. C. J.; Sawatzky, G.; Deliefde, H. J.; Jellinek, F *J. Organomet. Chem.* **1974**, *76*, C4–C6.
(26) Steyer, A.; Guenoun, P.; Beysens, D.; Knobler, C. M. *Phys. Rev. B* **1990**, *42*, 1086–1089.
(27) Barrow, M. S.; Jones, R. L.; Park, J. O.; Srinivasarao, M.; Williams, P. R.; Wright, C. J. *Spectrosc. Int. J.* **2004**, *18*, 577–585.
(28) Zhao, H. J.; Shen, Y. M.; Zhang, S. Q.; Zhang, H. M. *Langmuir* **2009**, *25*, 11032–11037.
(29) Jiang, P.; Bertone, J. F.; Colvin, V. L. *Science* **2001**, *291*, 453–457.